

Ginsenoside Rg₃ Inhibits Human Kv1.4 Channel Currents by Interacting with the K531 Residue

Jun-Ho Lee, Byung-Hwan Lee, Sun-Hye Choi, In-Soo Yoon, Mi Kyung Pyo, Tae-Joon Shin, Woo-Sung Choi, Yoong-Ho Lim, Hyewhon Rhim, Kwang Hee Won, Yong Whan Lim, Han Choe, Dong-Hyun Kim, Yang In Kim, and Seung-Yeol Nah

Ginsentology Research Laboratory and Department of Physiology, College of Veterinary Medicine, Konkuk University, Seoul Korea, 143-701 (J.-H.L., B.-H.L., S.-H.C., I.-S.Y., M.K.P., T.-J.S., W.-S.C., S.-Y.N.); Bio/Molecular Informatics Center, Konkuk University (Y.-H.L); Life Science Division, KIST, Seoul Korea 130-701 (H.R.); Department of Physiology and Research Institute for Biomacromolecules, University of Ulsan College of Medicine, Seoul 138-736, Korea (K.H.W., Y.W.L., H.C.); College of Pharmacy Kyung Hee University, 130-701, Korea (D.-H.K); Department of Physiology, Korea University College of Medicine, Seoul 136-705, Korea (Y.I.K.)

Running Title

Ginsenoside interaction site in human Kv1.4 channels

***Correspondence to:**

Prof. Seung-Yeol Nah, Ginsentology Research Laboratory and Department of Physiology, College of Veterinary Medicine, Konkuk University, Seoul 143-701 Korea.

Tel: 82-2-450-4154; Fax: 82-2-450-3037

Email: synah@konkuk.ac.kr

The abbreviations used are: Rg₃, ginsenoside Rg₃ (20-S-protopanaxadiol-3-[O-β-D-glucopyranosyl (1→2)-β-glucopyranoside]); Kv, voltage-gated K⁺ channel; TEA, tetraethylammonium.

Manuscript information

The number of text pages: 34

The number of table: 2

The number of figures: 5

The number of words in abstract: 250

The number of words in introduction: 327

The number of words in discussion: 1515

ABSTRACT

Recently we demonstrated that the 20(*S*) but not the 20(*R*) form of ginsenoside Rg₃ inhibited K⁺ currents flowing through Kv1.4 (hKv1.4) channels expressed in *Xenopus* oocytes, pointing to the presence of specific interaction site(s) for Rg₃ in the hKv1.4 channel. In the current study, we sought to identify this site(s). To this end, we first assessed how point mutations of various amino acid residues of the hKv1.4 channel affected inhibition by 20(*S*)-ginsenoside Rg₃ (Rg₃). Mutation to K531Y of the K531 residue, which is known to be a key site for K⁺ activation and to be part of the extracellular tetraethylammonium (TEA) binding site, abolished the Rg₃ effect and made the Kv1.4 channel sensitive to TEA applied to the extracellular side of the membrane. Mutations of many other residues, including the pH sensitive-site (H507 to H507Q), were without any significant effect. We next examined whether K⁺ and TEA could alter the effect of Rg₃ and *vice versa*. We found that: 1) raising [K⁺]_o reduced the inhibitory effect of Rg₃ on hKv1.4 channel currents, while Rg₃ shifted the K⁺ activation curve to the right and 2) TEA caused a rightward shift of the Rg₃ concentration-response curve of wild-type hKv1.4 channel currents, whereas Rg₃ caused a rightward shift of the TEA concentration-response curve of K531Y mutant channel currents. The docked modeling revealed that K531 residue plays a key role in forming hydrogen bonds between Rg₃ and hKv1.4 channels. These results indicate that Rg₃ inhibits the hKv1.4 channel current by interacting with residue K531.

Voltage-gated K^+ (Kv) channels play critical roles in a wide variety of physiological processes, including the regulation of neurotransmitter release, neuronal excitability, heart rate, muscle contraction, hormone secretion, epithelial electrolyte transport, cell volume, and cell proliferation in neuronal and non-neuronal cells (Hille, 2001). Kv channels consist of tetramers of pore-forming $Kv\alpha$ and auxiliary $Kv\beta$ subunits (Hille, 2001). The $Kv\alpha$ subunit is composed of six α -helical transmembrane segments (S1-S6). The S4 segment acts as the voltage-sensing apparatus of the K^+ channel (Hille, 2001), while the pore-forming S5-S6 segments constitute a selectivity filter and govern voltage-dependent increases in K^+ permeability. Site-directed mutagenesis studies using $Kv\alpha$ subunits have clarified the detailed action and binding sites of various drugs that regulate Kv channel activity (Hille, 2001). Some Kv channel α subunits exhibit transient A-type K^+ currents and N-type inactivation, and others, long-lasting delayed rectifying C-type K^+ currents and C-type inactivation, depending on their channel conductance and gating characteristics (Patel and Campbell, 2005).

Ginseng, the root of *Panax ginseng* C.A. Meyer, is well known in herbal medicine as a tonic and restorative agent, and it is consumed widely around the world. The molecular bases of ginseng's actions are largely unknown. Numerous reports have suggested that the main molecular ingredients responsible are ginsenosides (also called ginseng saponins), amphiphilic molecules consisting of a hydrophobic aglycone backbone (a hydrophobic four-ring steroid-like structure) linked to monomeric, dimeric

or tetrameric hydrophilic carbohydrate side chains (Fig. 1) (Nah, 1997). However it is unclear how ginsenosides produce their pharmacological effects. Recently we reported that ginsenoside Rg₃ (20-*S*-protopanaxadiol-3-[O-β-D-glucopyranosyl (1→2)-β-glucopyranoside]) (Rg₃) had an inhibitory effect on voltage-dependent human Kv1.4 (hKv1.4) channel activity expressed in *Xenopus laevis* oocytes (Jeong et al., 2004). In this report we present evidences that Rg₃ interacts with residue K531 to inhibit the channel currents. In addition, the docked modeling studies using hKv1.4 channels support that K531 residue plays an important role in the Rg₃-mediated regulations of hKv1.4 channel by forming hydrogen bonds between Rg₃ and hKv1.4 channels.

Materials and Methods

Materials Ginsenosides were kindly provided by the Korean Ginseng Cooperation (Taejon, Korea). The cDNA for human K⁺ channel Kv1.4 (Gene bank ID: NM_002233) was kindly provided by Dr. Pongs (University of Hamburg, Germany). Other agents were purchased from Sigma-Aldrich (St. Louis, MO, USA).

Preparation of *Xenopus* oocytes and microinjection *Xenopus laevis* frogs were purchased from Xenopus I (Ann Arbor, MI, USA). Their care and handling were in accordance with the highest standards of institutional guidelines. For isolation of

oocytes, frogs were anesthetized with an aerated solution of 3-amino benzoic acid ethyl ester and the ovarian follicles were removed. The oocytes were separated with collagenase followed by agitation for 2 h in Ca^{2+} -free medium containing 82.5 mM NaCl, 2 mM KCl, 1 mM MgCl_2 , 5 mM HEPES, 2.5 mM sodium pyruvate, 100 units/ml penicillin and 100 $\mu\text{g/ml}$ streptomycin. Stage V-VI oocytes were collected and stored in ND96 medium (in mM: 96 NaCl, 2 KCl, 1 MgCl_2 , 1.8 CaCl_2 , and 5 HEPES, pH 7.5) supplemented with 0.5 mM theophylline and 50 $\mu\text{g/ml}$ gentamicin. The oocyte-containing solution was maintained at 18°C with continuous gentle shaking and renewed every day. Electrophysiological experiments were performed within 5-6 days of oocyte isolation, with chemicals applied to the bath. For K^+ channel experiments, Kv channel-encoding cRNAs (40 nl) were injected into the animal or vegetal pole of each oocyte one day after isolation, using a 10 μl microdispenser (VWR Scientific, San Francisco, CA, USA) fitted with a tapered glass pipette tip (15-20 μm in diameter) (Lee et al., 2005).

Site-directed mutagenesis of the Kv1.4 α subunit and *in vitro* transcription of Kv1.4 channel cDNAs Single or double amino acid substitutions were made using a QuikChangeTM XL Site-Directed Mutagenesis Kit (Stratagene, La Jolla, CA, USA), along with Pfu DNA polymerase and sense and antisense primers encoding the desired

mutations. Overlap extension of the target domain by sequential polymerase chain reaction (PCR) was carried out according to the manufacturer's protocol. The final PCR products were transformed into *E. coli* strain DH5 α , screened by PCR and confirmed by sequencing of the target regions. The mutant DNA constructs were linearized at their 3' ends by digestion with *Xho*I, and run-off transcripts were prepared using the methylated cap analog, m⁷G(5')ppp(5')G. The cRNAs were prepared using a mMessage mMachine transcription kit (Ambion, Austin, TX, USA) with T7 RNA polymerase. The absence of degraded RNA was confirmed by denaturing agarose gel electrophoresis followed by ethidium bromide staining. Similarly, recombinant plasmids containing Kv channel cDNA inserts were linearized by digestion with the appropriate restriction enzymes, and cRNAs were obtained using the mMessage mMachine *in vitro* transcription kit with SP6 RNA polymerase or T7 polymerase. The final cRNA products were resuspended at a concentration of 1 μ g/ μ l in RNase-free water, and stored at -80°C (Lee et al., 2005).

Data recording A custom-made Plexiglas net chamber was used for two-electrode voltage-clamp recordings as previously reported (Lee et al., 2005). The oocytes were impaled with two microelectrodes filled with 3M KCl (0.2-0.7 M Ω), and electrophysiological experiments were carried out at room temperature using an Oocyte Clamp (OC-725C, Warner Instruments, Hamden, CT, USA). Stimulation and data

acquisition were controlled with a pClamp 8 (Axon Instruments, Union City, CA, USA). For most electrophysiological experiments, oocytes were perfused initially with ND96 solution (in mM: 96 NaCl, 3 KCl, 2 CaCl₂, 5 HEPES, pH 7.4 with NaOH) and control current recordings were obtained. To measure K⁺ activation of the Kv1.4 channel, a solution was applied in which the NaCl was replaced with various concentrations of KCl. In all cases the solution was perfused at a flow rate of ~3 ml/min, and the system was allowed 30 to 60 s to reach steady state prior to current recording. The oocytes were then clamped at a holding potential of -80 mV, membrane potential was depolarized to +50 mV for 500 ms every 10 s, and currents were recorded.

Homology modeling. A homology model of the hKv1.4 was built on the basis of the 2.9 Å crystal structure of the rat Kv1.2 channel (PDB ID code: 2A79), using the homology modeling program, MODELLER 8v2 (Sali and Blundell, 1993). Sequence alignment was carried out using the AlignX module of the Vector NTI (Lu and Moriyama, 2004). A stretch of amino acids in the Kv1.2 channel corresponding to the region from M438 to T571 in hKv1.4 was chosen as the template for homology modeling, because the other regions had structures missing in the PDB file. The chosen region contained the pore and its neighboring areas, and the sequence identity between hKv1.4 with rat Kv1.2 through this region was ~90%. The homotetrameric structure

was restrained to maintain symmetry during homology modeling. A total of 200 structures were generated, and the one with the lowest DOPE score from MODELLER was chosen for further minimization. Hydrogen atoms were added to the homology model using Sybyl v7.0 (Tripos Inc., St. Louis, MO, USA). The homology model structure was energy-minimized using the Tripos forcefield protocol in Sybyl. The same strategies were used to generate a homology model of K531Y.

Virtual docking. The structure of Rg₃ was constructed using Chemdraw ultra 8.0 (Cambridgesoft, Cambridge, MA, USA) and converted to a 3-dimensional model and energy minimized using Chem3D ultra 8.0 (Cambridgesoft, Cambridge, MA, USA), followed by a second round of energy minimization using Sybyl forcefield. The virtual dockings of Rg₃ to the homology model of hKv1.4 wild-type and K531Y mutant channels were performed using GOLD v3.0 (The Cambridge Crystallographic Data Centre, Cambridge, UK), a program that uses stochastic genetic algorithms for conformational searching (Verdonk et al., 2003). The K531 residues in each of the four subunits were designated as the active site residues, and the active radius was set as 10 Å from the active site residues. The docked models with the best GOLD scores were selected for final complex structural analysis. The interactions between the ligand and each homology model were examined using the SILVER tool of the GOLD software

package. All structural figures were prepared using PyMol v0.98 (DeLano Scientific LLC, San Francisco, CA, USA).

Data analysis To obtain the concentration-response curve of the effect of Rg₃ on the K⁺ current from the hKv1.4 channel, the peak amplitudes at different concentrations of Rg₃ were plotted, and Origin software (Origin, Northampton, MA, USA) was used to fit the plot to the Hill equation: $y/y_{\max} = [A]^{nH}/([A]^{nH} + [IC_{50}]^{nH})$, where y is the peak current at a given concentration of Rg₃, y_{\max} is the maximal peak current, IC_{50} is the concentration of Rg₃ producing a half-maximal effect, $[A]$ is the concentration of Rg₃, and nH is the Hill coefficient. All values are presented as means \pm S.E.M. The significance of differences between mean control and treatment values was determined using Student's t -test. $P < 0.05$ was considered statistically.

Results

Rg₃ inhibits hKv1.4 channel currents more potently than other ginsenosides.

Using the two-electrode voltage-clamp technique we recorded hKv1.4 channel currents from *Xenopus* oocytes injected with cRNA encoding the hKv1.4 channel protein. To elicit the currents, we applied a voltage step (500-ms duration) to +50 mV at 10-s intervals from a holding potential of -80 mV. The currents evoked by this voltage-clamp

protocol were transient A-type K^+ currents that decayed rapidly (Fig. 1B, *inset*) (Gomez-Hernandez et al., 1997). Rg_3 , at 100 μ M inhibited the hKv1.4 channel currents by an average of 65%, and other ginsenosides (Rb_1 , Rc , Rd , Rf , Rg_1 , Rh_2 , CK) were much less effective (Fig. 1B). The Rg_3 current effect was concentration-dependent (Fig. 2A) and reversible (data not shown). The IC_{50} value and Hill coefficient were 32.6 ± 2.2 μ M and 1.59 ± 0.13 , respectively (Table 1).

To assess the effect of Rg_3 on the current-voltage (I-V) relationship, we constructed I-V curves with and without Rg_3 in the bath. The current responses evoked by voltage steps (i.e., a series of voltage pulses of 500-ms duration given in 10-mV increments and 10-s intervals from the holding potential of -80 mV) were used to construct the I-V curve. In the absence of Rg_3 , hKv1.4 currents were elicited by voltage pulses more positive than -40 mV, and current amplitude increased linearly with further depolarization (Fig. 2D). The presence of Rg_3 reduced current amplitude over the entire voltage range in which the current was activated (Fig. 2D).

The K531Y substitution affects Rg_3 inhibition of channel current. Previous works showed that Rg_3 inhibited hvKv1.4 channel current in a stereospecific manner (Jeong., 2004) and that Rg_3 regulates 5-HT_{3A} receptor channel activity through interaction with amino acid residues in the channel pore region (Lee et al., 2007). We

therefore hypothesized that Rg₃ might have a specific interaction site(s) on the hKv1.4 channel and that Rg₃ interaction site(s) with the hKv1.4 channel might be related with channel pore region. To identify that site(s), we first made the following changes by site-directed mutations in channel pore regions: channel pore sites (S510 to S510K, D513 to D513Q, V525 to V525L and V535 to V535Q), outer pore sites (K531 to K531A, P532 to P532A, I533 to I533A, T534 to T534A and V535 to V535A). Next, we also constructed mutant channels as follows: N-glycosylation site (N352 to N353Q) (Watanabe et al., 2004), voltage sensor site (R447 to R447C and R450 to R450C) (Fedida and Hesketh, 2001), voltage shift sites (L478 to L478F and G548 to G548P) (Judge et al., 1999; Magidovich and Yifrach, 2004), pH sensitive site (H507 to H507Q) (Claydon et al., 2004) and C-type inactivation site (V560 to V560A) (Bett and Rasmusson, 2004). We found that one of outer pore residues K531A substitution significantly attenuated Rg₃ inhibition of the hKv1.4 channel currents (Fig. 2A), while the other changes had no significant effects (Table 1). These results showed a possibility that Rg₃ regulates hKv1.4 channel activity by interacting with K531, which is also known as one of K⁺ activation sites. Therefore, we constructed mutant channels at K⁺ activation sites (K531 to K531Y, I533 to I533M, and K531-I533 to K531Y-I533M) (Pardo et al., 1992; Claydon et al., 2004). We found that the K531Y substitution and the

K531Y-I533M double substitution almost abolished Rg₃ inhibition of the hKv1.4 channel currents (Fig. 2B-D). These results indicate that Rg₃-induced regulation of hKv1.4 channel activity is closely related with K531 residue.

Extracellular K⁺ and Rg₃ antagonize each other's effect on hKv1.4 channel currents. If indeed Rg₃ produces its effect by interacting with K531, the K⁺ activation site, an increase in extracellular [K⁺]_o would compete with Rg₃ for K531 and thus inhibit the action of the ginsenoside. Conversely, Rg₃ would inhibit K⁺ activation by competing with K⁺ for K531. We found that extracellular K⁺ and Rg₃ indeed antagonized each other's effect. Figure 3A-C shows that raising extracellular [K⁺]_o inhibited the effect of Rg₃ (IC₅₀ of extracellular K⁺ for the Rg₃ effect: 6.4 ± 2.9 mM), while Figure 3D shows that Rg₃ (100 μM) inhibited the effect of K⁺, thus shifting the K⁺ activation curve to the right (EC₅₀s of K⁺ before and after Rg₃ treatment: 4.2 ± 0.9 mM and 9.2 ± 1.5 mM, respectively; *P* < 0.01). These findings, confirm that Rg₃ competes with extracellular [K⁺] for the K531 residue.

TEA and Rg₃ inhibit each other's effect on hKv1.4 channel currents. Residue K531 is also known to form a part of the extracellular binding site for TEA (Heginbotham and Mackinnon, 1992; Gomez-Hernandez et al., 1997). We therefore reasoned that, if Rg₃ produced its effect by interacting with K531, extracellular

application of TEA should antagonize the effect of Rg₃ on channel currents, and conversely, Rg₃ should antagonize the TEA effect. To test these possibilities we used oocytes expressing wild-type or K531Y mutant hKv1.4 channels, because extracellularly applied TEA binds to both types of channel but only inhibits the mutant channels (Fig. 4A; IC₅₀: 26.5 ± 2.6 μM). Fig. 4B shows that TEA had no effect by itself on wild-type hKv1.4 channel currents, but that it inhibited the action of Rg₃, thus causing the Rg₃ concentration-response curve to shift to the right (IC₅₀s of Rg₃ before and during 10-μM TEA treatment: 35.1 ± 3.6 μM and 93.1 ± 6.7 μM, respectively; *P* < 0.001). Conversely Rg₃ antagonized the effect of TEA on K531Y channel currents, causing a rightward shift of the TEA concentration-response curve (IC₅₀'s of TEA before and during 100-μM Rg₃ treatment: 23.3 ± 2.7 μM and 40.1 ± 7.1 μM, respectively; *P* < 0.01) (Fig. 4C). These results lend further support to the hypothesis that Rg₃ interacts with K531 to inhibit hKv1.4 channel currents.

Docked modeling of interactions between Rg₃ and the hKv1.4 channel. To further examine the possible interaction mode between Rg₃ and the hKv1.4 channel, we carried out homology modeling of wild-type and K531Y mutant hKv1.4 channels. Our model was generated using the MODELLER program and the crystal structure of hKv1.2. Virtual docking of Rg₃ to the homology models was performed using the

docking program, GOLD. Interestingly, the best-fit docking results showed that Rg₃ forms six hydrogen bonds with wild-type hKv1.4 channels but only two hydrogen bonds with K531Y mutant channels (Fig. 5 and Table 2). In the wild-type channel, the first carbohydrate coupled to the Rg₃ backbone forms two hydrogen bonds with K531 of domain I (designated as Roman numeral I) and one hydrogen bond with H507 (IV). The second carbohydrate of Rg₃ forms one hydrogen bond with K531 (I), one hydrogen bond with T505 (I) and one hydrogen bond with H507 (I). In the K531Y mutant channel, the second carbohydrate of Rg₃ forms one hydrogen bond with Y531 (I) and the first carbohydrate of Rg₃ forms a hydrogen bond with H507 (IV) (Fig. 5 and Table 2). Notably, the wild-type Kv1.4 channel pore is blocked by the hydrophobic triterpenoid backbone moiety of Rg₃. The mutant channel is also blocked by Rg₃, but the low affinity of Rg₃ to the mutant channel (inferred from the small number of hydrogen bonds) might result in ineffective blocking of the mutant channel by Rg₃, thus accounting for the inability of Rg₃ to inhibit K531Y mutant channel currents.

Discussion

The Kv1.4 channel is a transient A-type or rapidly inactivating Kv channel. Kv1.4 channels are mainly located at axon and pre-synaptic terminals (Cooper et al.,

1998; Alonso and Widmer, 1997; Hoffman and Johnston, 1998; Adams et al., 2000), and function to modulate action potential waveforms and neurotransmitter release (Debanne et al., 1997; Jackson et al., 1991). They also affect the amplitude of the plateau phase and duration of action potentials in ventricular myocytes (Campbell et al., 1993; Patel and Campbell, 2005). Thus, these channels are one of the targets of drugs for treatment of pathologic conditions including cardiac arrhythmia. We previously demonstrated that Rg₃ regulated hKv1.4 channel currents in a stereospecific manner (Jeong et al., 2004). However, very little was known of its molecular mechanism of action.

In the present study we observed that mutation of K531 to K531A or K531Y, as well as raising extracellular [K⁺]_o from 3 to 99 mM, attenuated or almost abolished Rg₃ inhibition of hKv1.4 channel currents. These results show a possibility that Rg₃ might interact with the K⁺ activation sites, H507, K531, and I533 (Pardo et al., 1992; Claydon et al., 2004). To test these possibilities, we examined the effects of Rg₃ on H507Q, K531Y, I533M and K531Y-I533M channels. As shown in Figure 2, Rg₃ did not inhibit K531Y and K531Y-I533M channels even at high concentrations, whereas its effect on H507Q and I533M mutant channels was similar to that seen with wild-type channels (Table 1). These results indicate that although both H507 and I533 are involved in K⁺ activation (Pardo et al., 1992; Claydon et al., 2004), they are not

involved in Rg_3 regulation of channel activity. This view was supported by the results from our double mutation experiments. Furthermore, mutations in the channel pore region, pH-sensitive sites, voltage sensor and other regulatory sites did not affect Rg_3 inhibition (Table 1). Interestingly, Rg_3 is not structurally similar to TEA, a well-known K^+ channel blocker that can function on either side of the cell membrane. In contrast to TEA, Rg_3 does not have any charged groups apart from the hydroxyls of its carbohydrate and backbone structures (Fig. 1A). Despite the structural difference between Rg_3 and TEA, we found that the K531Y mutation of amino acid 531, which forms part of the external TEA interaction site, almost abolished Rg_3 inhibition of the channel currents. We also showed that Rg_3 competes with TEA for inhibition of K531Y channel currents (Fig. 4B) and vice versa (Fig. 4C). Interestingly, the rightward shift of the Rg_3 concentration-response curve caused by TEA in wild-type channels was stronger than that of the TEA concentration-response curve caused by Rg_3 in K531Y channels. Thus by making use of the fact that K531Y channels are sensitive to TEA whereas wild-type channels are not, we were able to demonstrate that Rg_3 may be an allosteric interaction site for TEA and Rg_3 . However, it is unlikely that Rg_3 exhibits an allosteric interaction with TEA on the intracellular surface of the channel since we have shown that Rg_3 regulates channels from the outside not the inside in out-side out patch

clamp experiments (Lee et al., 2004).

MacDonald et al (1998) showed that *n*-alkyl sulphate anions but not TEA inhibit wild-type rat Kv1.4 channel currents and that mutation of K533 to K533Y rendered channels sensitive to TEA but insensitive to *n*-alkyl sulphate anions. This indicates that K533 may play a role in *n*-alkyl sulphate anion-mediated Kv1.4 channel regulation via the external TEA interaction site. In addition, Zaks-Makhina et al. (2004) and Salvador-Recatala et al. (2006) have studied a neuroprotective compound, called 48F10, from yeast. They showed that 48F10 inhibited R476Y mutant rat Kv1.5 channel currents, (R476 is analogous to K531 in hKv1.4 channel) and wild-type rat Kv2.1 channel currents via the external TEA interaction site, since the presence of external TEA greatly reduced 48F10 current inhibition. Taken together, the previous and present observations raise the possibility that a lysine or analogous amino acid residue in the outer pores of subsets of Kv channels not only forms part of the external TEA interaction site but also plays a role as an allosteric interaction or overlapping site for TEA and certain other compounds.

Ginsenosides have effects on multiple targets (Attele et al., 1999). We and others have reported that ginsenosides, including Rg₃, also act on various ion channels at pre- and post-synaptic sites in the nervous systems and inhibit neurotransmitter release (Choi

et al., 2003; Kim et al., 2002; Lee et al., 2005; Liu et al., 2001; Nah et al., 1995; Sala et al., 2002; Tachikawa et al., 2001). Thus it appears that ginsenosides show a low degree of selectivity for ion channels compared to drugs or toxins that act on particular ion channels. However, we were not able to clearly define and comprehend the molecular mechanisms underlying ginsenoside-mediated regulation of multiple ion channels. We demonstrated that Rg₃ regulates 5-HT_{3A} receptor channel activity in the open state through interactions with amino acids such as V291, F292 and I295 in the gating pore region of transmembrane domain 2 (Lee et al., 2007). In the present study, we found that Rg₃ regulates Kv1.4 channel activity through interaction with the outer pore K531 residue and may interact allosterically with the external TEA binding site. Thus Rg₃ affects 5-HT_{3A} receptors and Kv1.4 channel activity via different interaction sites and different modes of regulation.

We next sought to examine the possible mechanisms underlying Rg₃-induced hKv1.4 channel activity regulation. As shown in Figure 1A, Rg₃ consists of a carbohydrate portion, a steroid backbone and an alkene side chain. To determine how Rg₃ interacts with Kv1.4 channels, we performed docked modeling experiments using wild-type and K531Y mutant channels. Our docked modeling study revealed that the two carbohydrates of Rg₃ could form six hydrogen bonds with residues T505 (I), H507

(I), H507 (IV) and K531 (I) in the wild-type channel. We previously demonstrated that Rg₃ regulates ligand-gated ion channels at the extracellular but not intracellular side using out-side out patch clamp method (Lee et al., 2004) and that modifications or removal of the carbohydrate portion of Rg₃ abolished Rg₃-mediated ion channel regulations, but at the time we were unable to explain exactly how Rg₃ regulates ion channel activity from the extracellular side and the carbohydrate portion of Rg₃ was involved in ion channel regulations (Kim et al., 2005). The modeling results in our present study suggest that the previously examined carbohydrate modifications might induce a conformational change in Rg₃ and/or prevent the formation of hydrogen bonds between Rg₃ and the critical residues. In the present study, the K531Y mutation was found to induce a conformational change in the channel protein (Fig. 5C), resulting in the formation of only two hydrogen bonds between Rg₃ and amino acid residues at the pore entryway. Thus, loss of hydrogen bonding between Rg₃ and the channel outer pore, whether through mutation or carbohydrate modification, appears to decrease the binding affinity of Rg₃, resulting in loss of Rg₃-induced channel regulation. Furthermore, as shown Figure 5B, our modeling revealed that the triterpenoid backbone of Rg₃ blocks the channel pore when the proper hydrogen bonds are formed; this may provide a secondary level of Rg₃-induced inhibition of outward K⁺ currents following

depolarization. Future studies will be necessary to determine the exact roles of the carbohydrates and/or triterpenoid backbone structures of Rg₃ in terms of Kv1.4 channel regulation.

We may ask whether the *in vitro* Rg₃ inhibition of the hKv1.4 channel applies also to its *in vivo* pharmacological effects. Ginseng has many beneficial effects on the cardiovascular systems (Gillis, 1997). Gao et al. (1992) have shown that ginsenoside administration via the intravenous route attenuates ischemic and reperfused arrhythmia in rats, and Yang et al. (1999) showed that ginsenoside administration via the intraperitoneal route attenuates myocardial reperfusion arrhythmia in rats fed a high cholesterol diet. Anti-arrhythmic agents such as quinidine block anti-arrhythmic effects on Kv1.4 and other cloned K⁺ channels (Wang et al., 2003) but we do not have any direct evidence that Rg₃-mediated Kv1.4 channel regulation can be used prophylactically or therapeutically against arrhythmia as quinidine can. More investigation is needed of the potential application of Rg₃ to heart dysfunction. In addition, Kim et al. (1999a and 1999b) showed that Rg₃ induced relaxation of the rat aorta via endothelium-dependent and -independent routes. They further showed that K⁺ channels in the rat aorta might be involved in the effect of Rg₃, since Rg₃-mediated aorta relaxation was achieved in a TEA-sensitive manner.

In summary, we have used site-directed mutagenesis, K⁺ activation experiments, and analysis of the external TEA interaction site to further characterize Rg₃ regulation of hKv1.4 channel activity. We found that the K531 residue of the hKv1.4 channel is involved in Rg₃-mediated Kv1.4 channel regulation and that Rg₃ may interact allosterically with the external TEA binding site via residue K531. Furthermore, in a molecular modeling we showed for the first time that two carbohydrates of Rg₃ interact with amino acid residues, including K531, through the formation of hydrogen bonds, which are decreased in K531Y mutant channels. These novel findings provide insight into the pharmacological basis of the beneficial effects of ginseng on cardiovascular systems.

References

- Adams JP, Anderson AE, Varga AW, Dineley KT, Cook RG, Pfaffinger PJ, and Sweatt JD (2000) The A-type potassium channel Kv4.2 is a substrate for the mitogen-activated protein kinase ERK. *J Neurochem* **75**:2277-2287
- Alonso G and Widmer H (1997) Clustering of Kv4.2 potassium channels in postsynaptic membrane of rat supraoptic neurons: an ultrastructural study. *Neuroscience* **77**:617-621
- Attele AS, Wu JA, Yuan CS (1999) Ginseng pharmacology: multiple constituents and multiple actions. *Biochem Pharmacol.* **58**: 1685-1693
- Bett GC and Rasmusson RL (2004) Inactivation and recovery in Kv1.4 K⁺ channels: lipophilic interactions at the intracellular mouth of the pore. *J Physiol* **556**:109-120
- Campbell DL, Rasmusson RL, Qu Y, Strauss HC (1993) The calcium-independent transient outward potassium current in isolated ferret right ventricular myocytes. I. Basic characterization and kinetic analysis. *J Gen Physiol* **101**:571-601
- Choi S, Lee JH, Oh S, Rhim H, Lee SM, and Nah SY (2003) Effects of ginsenoside Rg₂ on the 5-HT_{3A} receptor-mediated ion current in *Xenopus* oocytes. *Mol. Cells* **15**: 108-113.
- Claydon TW, Makary SY, Dibb KM, and Boyett MR (2004) K⁺ activation of

kir3.1/kir3.4 and kv1.4 K⁺ channels is regulated by extracellular charges. *Biophysical J* **87**:2407-2418

Cooper EC, Milroy A, Jan YN, Jan LY, and Lowenstein DH (1998) Presynaptic localization of Kv1.4-containing A-type potassium channels near excitatory synapses in the hippocampus. *J Neurosci* **18**:965-974

Dascal N (1987) The use of *Xenopus* oocytes for the study of ion channels. *CRC Crit. Rev. Biochem.* **22**: 317-387.

Debanne D, Guerineau NC, Gahwiler BH, and Thompson SM (1997) Action-potential propagation gated by an axonal I(A)-like K⁺ conductance in hippocampus. *Nature* **389**:286-289

Fedida D and Hesketh JC (2001) Gating of voltage-dependent potassium channels. *Prog Biophys Mol Biol* **75**:165-199

Gao BY, Li XJ, Liu L, and Zhang BH (1992) Effect of panaxatriol saponins isolated from *Panax notoginseng* (PTS) on myocardial ischemic arrhythmia in mice and rats. *Yao Xue Xue Bao.* **27**:641-644

Gillis, CN (1997) *Panax* ginseng pharmacology: a nitric oxide link? *Biochem Pharmacol.* **54**: 1-8.

Gomez-Hernandez JM, Lorra C, Pardo LA, Stuhmer W, Pongs O, Heinemann SH, and

- Elliott AA (1997) Molecular basis for different pore properties of potassium channels from the rat brain Kv1 gene family. *Pflugers Arch* **434**:661-668
- Hille B (2001) Ion channels of excitable membranes. *Sinauer Associates, Inc, Sunderland, MA*
- Heginbotham L and Mackinnon R (1992) The aromatic binding site for tetraethylammonium ion on potassium channels. *Neuron* **8**:483-491
- Hoffman DA and Johnston D (1998) Downregulation of transient K⁺ channels in dendrites of hippocampal CA1 pyramidal neurons by activation of PKA and PKC. *J Neurosci* **18**:3521-3528
- Jackson MB, Konnerth A, and Augustine GJ (1991) Action potential broadening and frequency-dependent facilitation of calcium signals in pituitary nerve terminals. *Proc Natl Acad Sci USA* **88**:380-384
- Jeong SM, Lee JH, Kim JH, Lee BH, Yoon IS, Lee JH, Kim DH, Rhim H, Kim Y, and Nah SY (2004) Stereospecificity of ginsenoside Rg₃ action on ion channels. *Mol Cells* **18**:383-389
- Judge SI, Monteiro MJ, Yeh JZ, and Bever CT (1999) Inactivation gating and 4-AP sensitivity in human brain Kv1.4 potassium channel. *Brain Res* **831**:43-54
- Kang DI, Lee JY, Yang JY, Jeong SM, Lee JH, Nah SY, and Kim Y (2005) Evidence that

the tertiary structure of 20(S)-ginsenoside Rg₃ with tight hydrophobic packing near the chiral center is important for Na⁺ channel regulation. *Biochem Biophys Res Commun* 333:1194-1201.

Kim JH, Hong YH, Lee JH, Kim DH, Jeong SM, Lee BH, Lee SM, and Nah SY (2005)

A role for the carbohydrate portion of ginsenoside Rg₃ in Na⁺ channel inhibition. *Mol Cells* 19:137-142

Kim ND, Kang SY, Kim MJ, Park JH, and Schini-Kerth VB (1999a) The ginsenoside

Rg₃ evokes endothelium-independent relaxation in rat aortic rings: role of K⁺ channels. *Eur J Pharmacol* 367: 51-57

Kim ND, Kang SY, Park JH, and Schini-Kerth VB (1999b) Ginsenoside Rg₃ mediates

endothelium-dependent relaxation in response to ginsenosides in rat aorta: role of K⁺ channels. *Eur J Pharmacol* 367: 41-49

Kim S, Ahn K, Oh TH, Nah SY, and Rhim H (2002) Inhibitory effect of ginsenosides on

NMDA receptor-mediated signals in rat hippocampal neurons. *Biochem. Biophys. Res. Commun.* 296: 247-254.

Lee JH, Jeong SM, Kim JH, Lee BH, Yoon IS, Lee JH, Choi SH, Kim DH, Rhim H,

Kim S, Kim JI, Jang CG, Song JH, and Nah SY (2005) Characteristics of ginsenoside Rg₃-mediated brain Na⁺ current inhibition. *Mol Pharmacol* 68:1114-1126

- Lee BH, Jeong SM, Ha TS, Park CS, Lee JH, Kim JH, Kim DH, Han JS, Kim, HC, Ko SR, and Nah SY (2004) Ginsenosides Regulate Ligand-gated Ion Channels from the Outside. *Mol Cells* **18**: 115-121
- Lee BH, Lee JH, Lee SM, Yoon IS, Lee JH, Choi SH, Pyo MK, Rhim H, Kim HC, Jang CG, Lee BC, Park CS, and Nah SY (2007) Identification of ginsenoside interaction sites in 5-HT_{3A} receptors. *Neuropharmacology* **52**: 1139-1150
- Liu D, Li B, Liu Y, Attele, AS, Kyle JW, and Yuan CS (2001) Voltage-dependent inhibition of brain Na⁺ channels by American ginseng. *Eur J Pharmacol* **413**: 47-54
- Lu G and Moriyama EN (2004) Vector NTI, a balanced all-in-one sequence analysis suite. *Briefings in bioinformatics* **5**:378-388
- Magidovich E and Yifrach O (2004) Conserved gating hinge in ligand- and voltage-dependent K⁺ channels. *Biochemistry* **43**:13242-13247
- McAllister RE and Noble D (1966) The time and voltage dependence of the slow outward current in cardiac Purkinje fibres. *J Physiol* **186**:632-662
- MacDonal S, Elliott AA, Harrold JA, and Elliott JR (1998) Influence of outer pore residue K533 on the inhibition of Kv1.4 potassium channels by n-alkyl sulphate anions. *Pflugers Arch.* **436**: 623-626
- Nah SY (1997) Ginseng : Recent Advances and Trends. *Kor. J. Ginseng Sci.* **21**: 1-12.

Nah, SY, Park, HJ, and McCleskey, EW. (1995) A trace component of ginseng that inhibits Ca^{2+} channels through a pertussis toxin-sensitive G protein. *Proc. Natl. Acad. Sci. USA* **92**: 8739-8743.

Patel SP and Campbell DL (2005) Transient outward potassium current, 'Ito', phenotypes in the mammalian left ventricle: underlying molecular, cellular and biophysical mechanisms. *J Physiol* **569**:7-39

Pardo LA, Heinemann SH, Terlau H, Ludewig U, Lorra C, Pongs O, and Stuhmer W (1992) Extracellular K^{+} specifically modulates a rat brain K^{+} channel. *Proc Natl Acad Sci USA* **89**:2466–2470

Sala F, Mulet J, Choi S, Jung SY, Nah SY, Rhim H, Valor LM, Criado M, and Sala S (2002) Effects of ginsenoside Rg_2 on human neuronal nicotinic acetylcholine receptors. *J. Pharmacol. Exp. Ther.* **301**: 1052-1059.

Sali A and Blundell TL (1993) Comparative protein modelling by satisfaction of spatial restraints. *J Mol Biol* **234**:779-815.

Salvador-Recatala V, Kim Y, Zaks-Makhina E, and Levitan ES (2006) Voltage-gated K^{+} channel block by catechol derivatives: defining nonselective and selective pharmacophores. *J Pharmacol Exp Ther.* **319**: 758-64.

Tachikawa E, Kudo K, Nunokawa M, Kashimoto T, Takahashi E, Kitakawa S (2001)

- Characterization of ginseng saponin ginsenoside-Rg₃ inhibition of catecholamine secretion in bovine adrenal chromaffin cells. *Biochem Pharmacol.* **62**: 943-951
- Verdonk ML, Cole JC, Hartshorn MJ, Murray CW, and Taylor RD (2003) Improved protein-ligand docking using GOLD. *Proteins* **52**:609-623
- Wang S, Morales MJ, Qu YJ, Bett GCL, Strauss HC, and Rasmussen RL (2003) Kv1.4 channel block by quinidine: evidence for a drug-induced allosteric effect. *J Physiol.* **546**: 387-401.
- Watanabe I, Zhu J, Recio-Pinto E, and Thornhill WB (2004) Glycosylation affects the protein stability and cell surface expression of Kv1.4 but Not Kv1.1 potassium channels. A pore region determinant dictates the effect of glycosylation on trafficking. *J Biol Chem* **279**:8879-8885
- Yang Y, He K, Wu T, Li Q, Zhang JS, and Fu ZG (1999) Effects of ginsenosides on myocardial reperfusion arrhythmia and lipid superoxidation in high cholesterol diet rats. *Shi Yan Sheng Wu Xue Bao.* **32**:349-352.
- Zaks-Makhina E, Kim Y, Aizenman E, and Levitan ES (2004) Novel neuroprotective K⁺ channel inhibitor identified by high-throughput screening in yeast. *Mol. Pharmacol.* **65**: 214-219

FOOTNOTES

This work was supported by grants to S. Y. Nah from the BK21 project and Korean Research Foundation Grant funded by MOEHRD (KRF-2005-015-E00222), the Neurobiology Research Program from MOST and KIST Core-Competence Program to H. Rhim as well as a grant (2007-307) to H. Choe from the Asan Institute for Life Science, Seoul, Korea. We thank Prof. O. Pongs for providing Kv1.4 channel cDNAs. J.-H.L. and B.-H.L. contributed equally to this work.

Figure legends

Fig. 1. Chemical structures of ginsenosides and effects of various ginsenosides on hKv1.4 channel currents. A, Ginsenosides differ in the three side chains attached to a common steroid-like ring. Abbreviations for carbohydrates are as follows: Glc, glucopyranoside; Ara (pyr), arabinopyranoside; Rha, rhamnopyranoside. Superscripts indicate the glucose ring carbon that links the two carbohydrates. B, Summary histograms showing the effects of various ginsenosides (100 μ M each) on the wild-type hKv1.4 channel current. *Inset*, Representative hKv1.4 channel currents elicited by 500-ms voltage steps to +50 mV from a holding potential of -80 mV, in the absence and presence of 100- μ M of ginsenosides Rh₂, Rg₃, and compound K (CK).

Fig. 2. Rg₃ effects on wild-type and mutant hKv1.4 channel currents. A, Concentration-response curves for Rg₃-induced inhibition of wild-type and mutant hKv1.4 channel currents. The same voltage protocol as in A was used to elicit the K⁺ currents. Amino acids in outer pore residues near selectivity filter were mutated into alanine. B, Representative wild-type and K531Y mutant hKv1.4 channel currents elicited in the absence and presence of various concentrations of Rg₃. C, Concentration-response curves for Rg₃-induced inhibition of wild-type and mutant hKv1.4 channel currents. D,

Current-voltage (I-V) relationships of wild-type and mutant hKv1.4 channels in the absence or presence of Rg₃. Voltage pulses of 500-ms duration were applied in 10-mV increments and at 10-s intervals from a holding potential of -80 mV. The peaks of the evoked currents, normalized to the peak current evoked by the voltage step to +60 mV in the absence of Rg₃, were used in the I-V plot. **P* < 0.01 compared with wild-type hKv1.4 channel.

Fig. 3. Mutual antagonistic actions of extracellular [K⁺] and Rg₃ on hKv1.4 channel currents. A, hKv1.4 channel currents evoked in 3-mM and 99-mM K⁺ by 500-ms voltage pulses to +50 mV from a holding potential of 0 mV, in the absence and presence of Rg₃. B, Plot showing the effect of extracellular [K⁺] on Rg₃ (100 μM) inhibition of the current. C, K⁺ current activation curves constructed from the currents evoked in the absence and presence of Rg₃. D, I-V plots for hKv1.4 channel currents obtained in 3- and 99-mM K⁺, in the absence and presence of Rg₃ (100 μM). Currents are normalized to that evoked in 3-mM K⁺ by the voltage step to +60 mV in the absence of Rg₃.

Fig. 4. Mutually antagonistic action of TEA and Rg₃ on wild-type and K531Y mutant hKv1.4 channel currents. A, Concentration-dependent effects of TEA on wild-type and

K531Y hKv1.4 channel currents. B, Concentration-response curves for Rg₃ inhibition of the wild-type hKv1.4 channel current in the absence and presence of TEA (10 μM). *Inset*, Representative K⁺ current traces from control oocytes (□) and oocytes treated with 100-μM Rg₃ + 10-μM TEA (○), or 100-μM Rg₃ alone (●). C, Concentration-response curves for TEA inhibition of K531Y channel currents evoked in the absence and presence of Rg₃ (100 μM). *Inset*, Representative K⁺ current traces from controls (□) and oocytes treated with 100-μM Rg₃ + 30-μM TEA (○), or 30-μM TEA alone (●).

Fig. 5. Theoretical docking of Rg₃ to wild-type and K531Y mutant Kv1.4 channels.

Hydrogen bonds are denoted as red broken lines. The Roman numerals in parenthesis indicate the number of the homotetramer subunit involved in the interaction. A, Structure of Rg₃. Glc, glucopyranoside. B, A docked model of wild-type Kv1.4 channel and Rg₃. Six hydrogen bonds are predicted to form between key residues and Rg₃, including three hydrogen bonds to K531(I) one hydrogen bond each to T505(I), His507(I), and H507(IV). The lower panel contains a 90-degree rotated view of the upper panel, showing that the Kv1.4 channel pore is predicted to be blocked by the hydrophobic triterpenoid moiety of the ginsenoside. C, A docked model showing binding of Rg₃ to the K531Y mutant channel. Only 2 hydrogen bonds form, one each to T531(I) and H507(IV) (see Table 2).

TABLE I

Effects of Rg₃ on wild-type and mutant hKv1.4 channels expressed in *Xenopus laevis* oocytes.
 Currents were elicited by single-step voltage pulses from -80 to +50 mV.

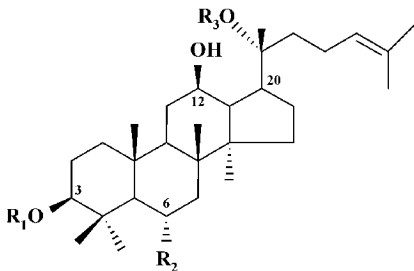
Type	IC ₅₀	V _{max}	n _H
Wild type	32.6 ± 2.2	75.4 ± 2.0	1.59 ± 0.13
N352Q	38.2 ± 3.5	81.2 ± 5.2	1.61 ± 0.22
R447C	30.6 ± 2.4	69.1 ± 2.1	1.35 ± 0.11
R450C	26.1 ± 1.1	91.8 ± 1.4	1.46 ± 0.07
L478F	36.5 ± 3.5	93.6 ± 3.3	1.16 ± 0.09
H507Q	34.4 ± 3.0	84.5 ± 2.8	1.34 ± 0.12
S510K	39.8 ± 1.6	83.7 ± 1.3	1.25 ± 0.04
D513Q	41.2 ± 3.3	88.4 ± 3.1	1.32 ± 0.21
V525L	38.5 ± 4.6	68.1 ± 3.1	1.12 ± 0.09
K531A	63.3 ± 9.4*	47.9 ± 3.2*	1.27 ± 0.12
K531Y	ND	ND	ND
P532A	44.6 ± 3.1	75.5 ± 2.1	1.31 ± 0.13
I533A	39.1 ± 7.0	72.6 ± 3.4	1.31 ± 0.12
I533M	35.5 ± 0.9	71.5 ± 1.8	1.36 ± 0.08
T534A	36.9 ± 1.6	87.6 ± 1.5	1.28 ± 0.11
V535A	41.6 ± 3.3	70.7 ± 2.0	1.37 ± 0.15
V535Q	36.2 ± 2.5	72.5 ± 4.5	1.24 ± 0.12
G548P	29.5 ± 5.6	69.5 ± 3.5	1.26 ± 0.23
V560A	35.6 ± 5.7	65.8 ± 4.1	1.34 ± 0.21
K531Y + I533M	ND	ND	ND

ND, not determined. *P < 0.01 compared with wild-type hKv1.4 channel

TABLE II
Modeled hydrogen bonds between hKv1.4 and Rg₃.

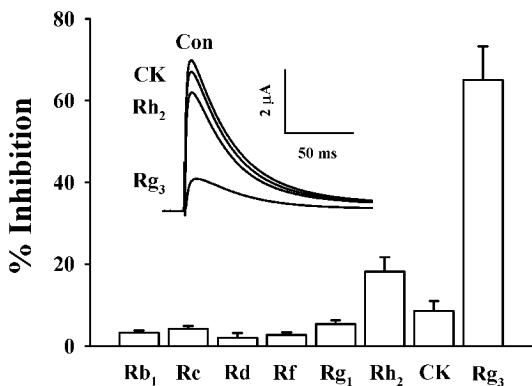
Type	Residue	Rg ₃	Distance (Å)
Wild-Type	K531 (I)	O3`	2.336
		O2`	2.543
		O2``	2.629
	T505 (I)	HO4``	2.604
	H507 (I)	O3``	3.288
	H507 (IV)	HO4`	2.695
K531Y	Y531 (I)	HO3``	2.022
	H507 (IV)	O3`	2.449

The Roman numerals in parenthesis indicate the subunit number of the homotetramer involved in the interaction. The ` and `` markings indicate the first and second carbohydrates of Rg₃, respectively (see Fig. 5A), and the adjacent numbers indicate the position of the relevant carbon in each carbohydrate ring.

A

Ginsenoside

	R ₁	R ₂	R ₃
Rb ₁	-Glc ₂ -Glc	-H	-Glc ₆ -Glc
Rc	-Glc ₂ -Glc	-H	-Glc ₆ -Ara(fur)
Rd	-H	-O-Glc ₂ -Rha	-Glc
Rf	-H	-O-Glc ₂ -Glc	-H
Rg ₁	-H	-O-Glc	-Glc
Rg ₃	-Glc ₂ -Glc	-H	-H
Rh ₂	-Glc	-H	-H
CK	-H	-H	-Glc

B**Fig. 1**

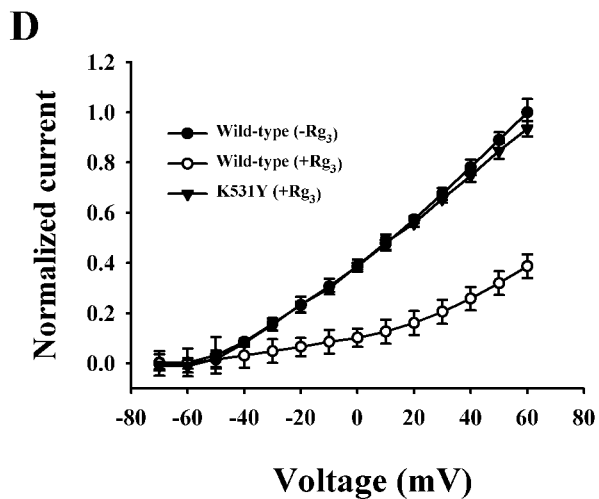
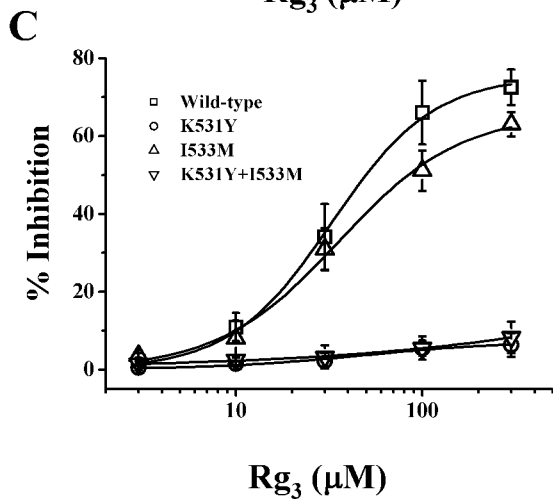
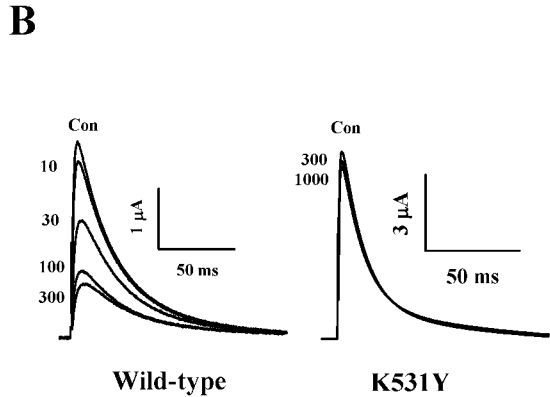
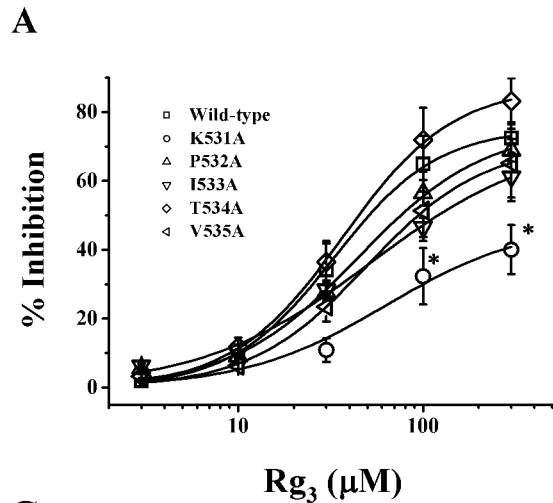


Fig. 2

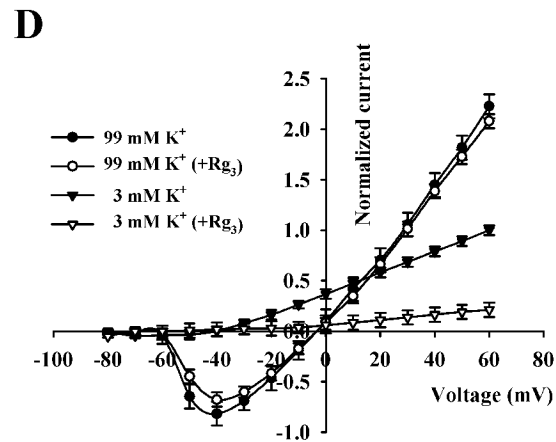
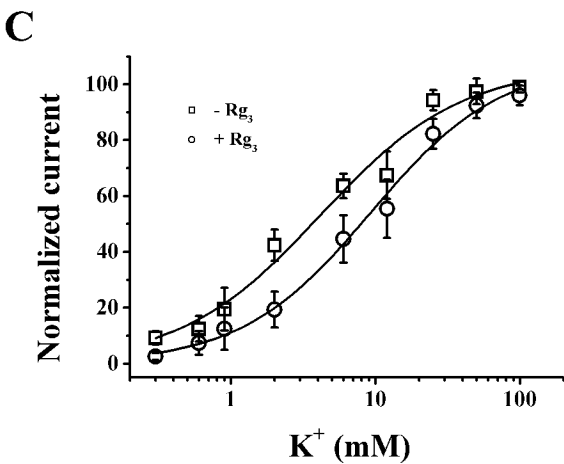
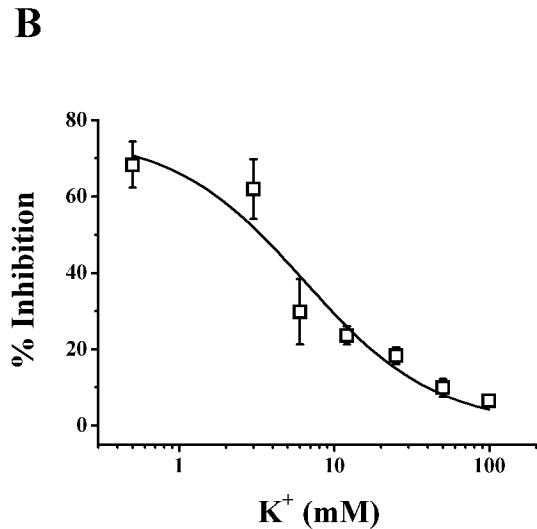
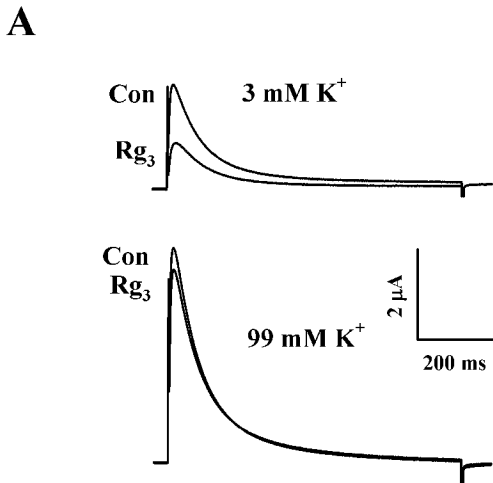
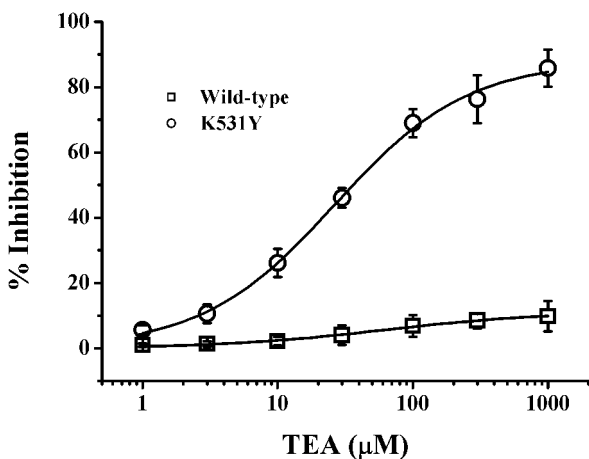
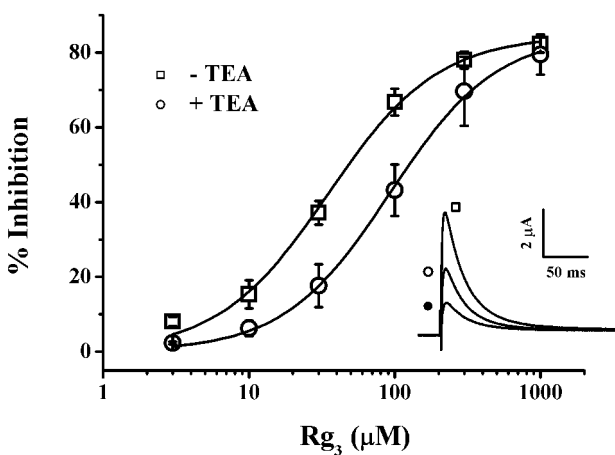
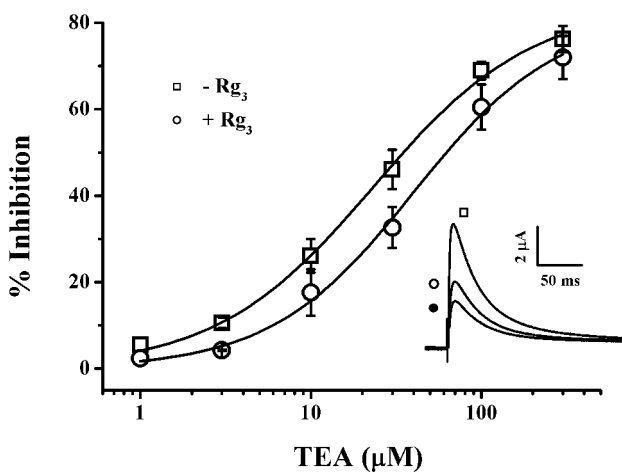
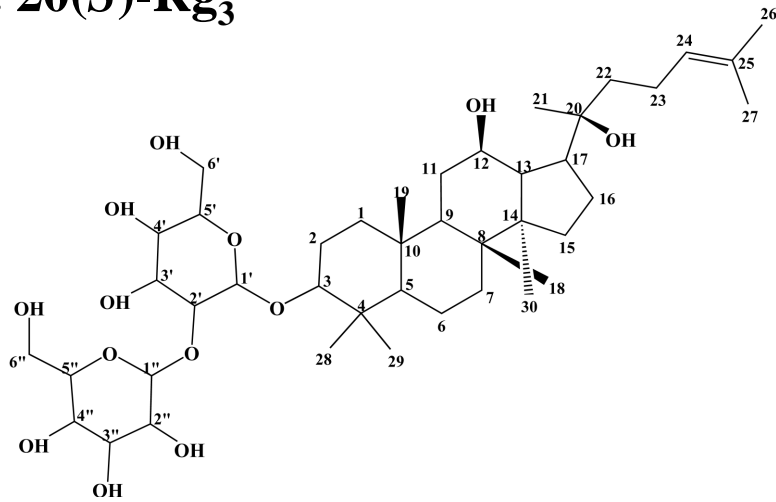


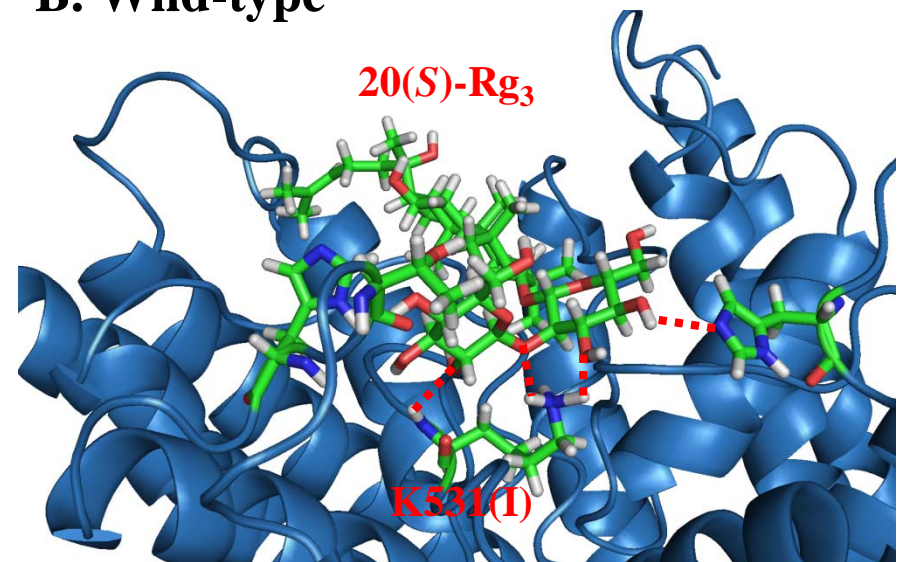
Fig. 3

A**B. Wild-type****C. K531Y****Fig. 4**

A. 20(S)-Rg₃



B. Wild-type



C. K531Y

